System Design for a Long-Line Quantum Repeater

Rodney Van Meter, *Member, IEEE*, Thaddeus D. Ladd, W.J. Munro, and Kae Nemoto

***Abstract*— We present a new control algorithm and system design for a network of quantum repeaters, and outline the end-to-end protocol architecture. Such a network will create long-distance quantum states, supporting quantum key distribution as well as distributed quantum computation. Quantum repeaters improve the reduction of quantum-communication throughput with distance from exponential to polynomial. Because a quantum state cannot be copied, a quantum repeater is not a signal amplifier. Rather, it executes algorithms for quantum teleportation in conjunction with a specialized type of quantum error correction called *purification* to raise the *fidelity* of the quantum states. We introduce our *banded* purification scheme, which is especially effective when the fidelity of coupled qubits is low, improving the prospects for experimental realization of such systems. The resulting throughput is calculated via detailed simulations of a long line composed of shorter hops. Our algorithmic improvements increase throughput by a factor of up to fifty compared to earlier approaches, for a broad range of physical characteristics.**

I. Introduction

QUANTUM computers exist, and have been used to solve small problems [1], [2]. The range of potential uses includes some important problems such as Shor's algorithm for factoring large numbers and physical simulations of quantum systems; for a few applications, quantum computers may exhibit exponential speedup over classical computers [3]–[5]. However, the engineering challenges of creating large-scale quantum computers are daunting [6], [7], and current capacities are only up to about 8-12 quantum bits, or *qubits* [8], [9]. Therefore, some researchers have suggested that networks of small quantum computers be used to overcome the limitations of individual machines, creating distributed quantum systems [10]–[15]. The goals of a quantum network are the same as any classical distributed system: to connect computational resources, data, or people so that the resulting system is more valuable than the sum of its parts. The distant systems may have access to different data, may provide different computational capabilities, or may simply increase total capacity.

The first real-world deployments of quantum networks have already begun. The first and most developed application is *quantum key distribution* (QKD), which uses a quantum channel and an authenticated (but not necessarily secret) classical channel to create shared, secret, random classical bits that can be used as a cryptographic key [16][1]. An experimental metropolitan-area QKD network has been developed and deployed in the Boston area [18], and similar efforts are underway in Japan [19] and Europe [20]. Efforts to extend these networks to wider areas are constrained by loss in the communication channel, which results in exponential decay in throughput as distance increases.

When the end points of a connection are far apart, the use of specialized devices called *quantum repeaters* may be required [21]–[26]. A quantum repeater is qualitatively different from a classical signal amplifier; it does not copy a quantum state or regenerate signal levels (as this is provably impossible in general [27]). Instead, quantum repeaters transfer quantum data via a distributed quantum algorithm called *teleportation* [28]–[30], which allows the transfer of a quantum state via classical communication. Experimental progress toward the realization of such repeaters has recently been reported [31], [32].

Teleportation consumes a special form of *entangled state* known as a *Bell pair*. In an entangled state, two quantum systems that may be physically separated share a non-local correlation that Einstein famously referred to as “spooky action at a distance”. QKD does not directly require entangled states. However, the distributed Bell pairs created by repeaters will enable long-distance QKD, and most other applications of distributed quantum computation will use distributed Bell pairs as well [13]–[15], [33].

We would like to have perfect Bell pairs to use for our distributed computations. Unfortunately, perfect systems do not exist, so we must concern ourselves with the *fidelity* of quantum states, a metric we will use to describe how near we are to perfect Bell states. The fidelity is defined as the probability that a perfect measurement of two qubits would show them to be in the desired Bell state. The fidelity is reduced by channel loss and imperfect control of qubits, but it may be improved by a form of error correction called *purification* [12], [34]–[37].

The primary contribution of this paper is the introduction of the *banded purification* algorithm, which improves the utilization of physical and temporal resources in a network of repeaters. Our simulations show that banded purification will improve performance by up to a factor of fifty compared to prior schemes. Banding restricts purification to using Bell pairs of similar fidelity, in order to improve both the probability of success of the purification and the resulting boost in fidelity

R. Van Meter is with Keio University and National Institute of Informatics, Tokyo, Japan (NII) (email: rdv@sfc.wide.ad.jp). K. Nemoto is with NII (email: nemoto@nii.ac.jp). T. D. Ladd is with NII and with Stanford University (email: tdladd@gmail.com). W.J. Munro is with Hewlett-Packard Laboratories, Bristol, UK and with NII (email: bill.munro@hp.com).

[1] Note that QKD does not completely solve the security problems created by Shor's quantum algorithm for factoring large numbers and finding discrete logarithms; Shor impacts public-key encryption (which is used in authentication mechanisms) and the Diffie-Hellman key agreement protocol. QKD provides key exchange, but requires authentication [17].

when it succeeds. We have characterized expected gains for some system engineering trade-offs. Our results increase the performance of the system and relax hardware constraints, improving the prospects for experimental implementation of wide-area quantum networks. We also provide a description of repeater operation as a network-centric layered protocol model, outlining the messages transferred, the need for layers to share an addressing scheme for qubits and the repeaters themselves, and buffer management.

Section II presents the basic operation of quantum repeaters. Section III outlines a layered protocol architecture to support these operations. Section IV describes prior work in scheduling purification, then presents our banded algorithm. Our simulation results are detailed in Section V, showing the improvement in performance using banding, as well as the hardware constraints and trade-offs we have identified. We conclude in Section VI.

II. Quantum Repeater Basics

A network of quantum repeaters supports distributed quantum computation by creating high-fidelity end-to-end Bell pairs. Once completed, these pairs can then be used to teleport application data, which is generally too valuable to risk in the error-prone process of hop-by-hop teleportation. Section I identified the three functions that a network of quantum repeaters must provide: a basic entangling mechanism, and the two distributed algorithms, purification and teleportation, which transform large numbers of short-distance, low-fidelity Bell pairs into smaller numbers of long-distance, high-fidelity pairs.

A quantum repeater, which we also call a *station*, is a small, special-purpose quantum computer, holding a few physical qubits that it can couple to a transmission medium. The hardware provides the basic capability of creating short-distance, low-fidelity (“base level”) Bell pairs via a physical entanglement mechanism [2]; the other two functions require classical communications and computation, and local quantum operations.

In classical packet-switched networks, an in-flight packet consumes resources such as buffer space, computation, and bandwidth only at its current location (modulo end-to-end reliable delivery considerations, such as TCP). Quantum repeaters, in contrast, involve widely distributed quantum computation; each station participates repeatedly in building an end-to-end distributed Bell pair, through purification and the use of teleportation known as *entanglement swapping*.

In this section, we first describe how the base-level Bell pairs are created over a single hop, then how Bell pair fidelity is improved at all distances by using purification. With this background, we turn to teleportation and entanglement swapping.

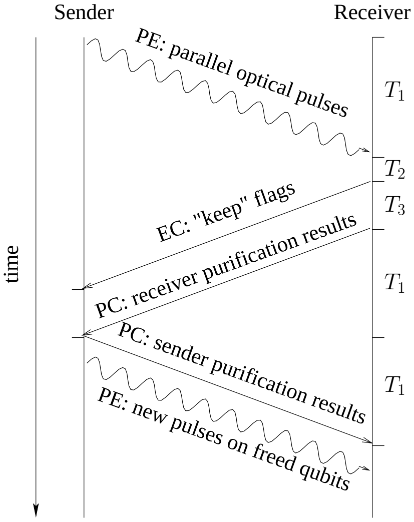
Sender
Receiver
time
PE: parallel optical pulses
T_1
T_2
EC: "keep" flags
T_3
PC: receiver purification results
T_1
PC: sender purification results
T_1
PE: new pulses on freed qubits

Fig. 1. Messaging sequence for the lowest level of Bell pair creation and purification.

A. Bell Pair Creation

Over distances greater than a few millimeters, the creation of Bell pairs is mediated by photons, which may be sent through free space or over a waveguide such as optical fiber. Schemes for Bell-pair creation may be divided very crudely into those that use very weak amounts of light – single photons, pairs of photons, or laser pulses of very few photons [22], [38]–[42] – and those that use laser pulses of many photons, which are called *qubus* schemes [24], [25], [43], [44]. Qubus repeaters, also known as “hybrid” repeaters because they utilize some analog classical characteristics of light in conjunction with the digital characteristics of qubits, are currently being developed by a multi-institution collaboration involving the authors. The methods of creating photons, performing entangling operations, and making measurements are different in each type of repeater, but at the level relevant for this paper the architectures are similar.

At the physical level, the relationship between the probability of successfully creating a Bell pair and the fidelity of the created pair is complex. Only Bell pairs with fidelity bounded well above 0.5 contain useful amounts of entanglement; as the fidelity degrades toward 0.5, we become unable to make use of the pair. Using the qubus scheme, the probability of successfully creating a Bell pair is high, but even when the operation succeeds the fidelity of the created Bell pair is low (these two parameters represent an engineering tradeoff we will not discuss here). For the parameter settings we have chosen, corresponding to the qubus scheme, Bell pairs are created with fidelities of 0.77 or 0.638 for 10km and 20km distances, respectively, and the creation succeeds on thirty-eight to forty percent of the attempts [25]. Methods for Bell pair creation that utilize single photons have much lower success probabilities, but create very high-fidelity Bell pairs when they do succeed.

Figure 1 shows the message sequence for creating base-level entangled pairs. The wavy lines in the figure (labeled PE, for

[2] When we speak of the “creation” and “destruction” of Bell pairs, we are referring the *state* of two qubits in separate repeaters; the physical qubits in the repeaters are not physically created or destroyed.

Physical Entanglement) indicate the optical pulses that interact directly with the qubits, while the straight lines are classical communication. At the sender, an optical pulse is entangled with each separate physical qubit, then multiplexed into the long-distance fiber. The pulses are very short compared to the propagation delay of tens to hundreds of microseconds (T_1 in the figure), so we can treat the pulses as effectively being instantaneous. Upon arriving at the receiver, the pulses are demultiplexed, and an attempt is made to entangle each one with a free qubit. Certain properties of the pulse are then measured [22], [39]–[41]. The measurement results tell us if the entangling operation succeeded. If so, we have created a *Bell pair*, entangling a qubit at the sender with a qubit at the receiver. The receiver prepares ACK/NAK "keep" flags for each qubit and sends them back to the sender, letting the sender know which operations succeeded. This measurement and flag preparation is T_2 in the figure and the return message is labeled EC (Entanglement Control).

B. Purification

If the two stations have successfully created more than one Bell pair, they can next begin the distributed quantum computation known as *purification*. Purification raises the fidelity of a Bell pair, essentially performing error correction on a test pattern, taking advantage of the specially-prepared initial state of the qubits. Purification takes two Bell pairs and attempts, via local quantum operations and classical communication, to combine them into one higher-fidelity pair, an operation that takes time T_3 in Figure 1.

Two facets of purification determine its efficiency: the quantum algorithm used on each pair of Bell pairs, for which there are several methods [45]–[47], and the *scheduling* [48]. Scheduling chooses which pairs to purify with each other, and has an enormous impact on the physical resources required and the rate at which the fidelity of a Bell pair grows. We will discuss scheduling in detail in Section IV. The quantum algorithm used on each pair may be chosen to be the same regardless of each pair's history, as in Refs. [45] and [46], but additional efficiency is gained by tracking the noise accumulated in each pair as it has developed in the repeater and changing the algorithm appropriately. If the noise of the two input Bell pairs is known, one of a small, finite set of possible algorithms may be chosen which minimizes the noise of the resulting purified pair [47]. We use such an approach for our offline simulations, assuming the noise expected from qubus-based hardware [25]. Such an approach is also possible in real time, but since we cannot directly measure the quantum parts of the system without disturbing the quantum state, the quantum state must be tracked by simultaneous classical calculations identical to our simulations.

Purifying two pairs always destroys one Bell pair and returns its physical resources to the pool of free qubits. If the operation fails, both pairs are freed for reuse, but if the operation succeeds, the resulting higher-fidelity pair is either kept to await more purification (if the target fidelity for this distance has not yet been reached) or is passed to the next higher level in the protocol stack. T_2 and T_3 are both small compared to T_1, so we will ignore them in this paper.

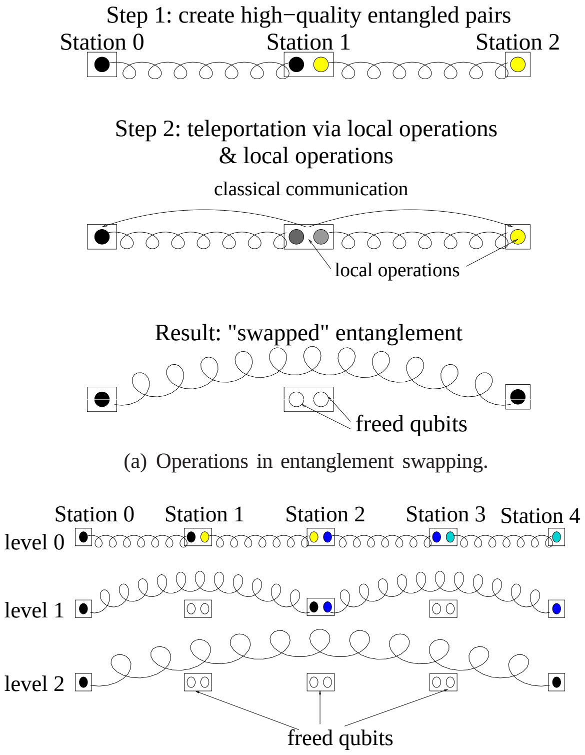
Step 1: create high−quality entangled pairs
Station 0
Station 1
Station 2
Step 2: teleportation via local operations
& local operations
classical communication
local operations
Result: "swapped" entanglement
freed qubits

(a) Operations in entanglement swapping.

(b) Three levels of entanglement swapping.

Fig. 2. Entanglement swapping. Spiral lines represent distributed Bell pairs, and straight lines are classical communication.

C. Teleportation and Swapping

The use of teleportation in repeaters, known as entanglement swapping, lengthens distributed Bell pairs by teleporting the state of one member of a Bell pair over progressively longer distances, until the pair stretches from end to end. Teleportation consumes Bell pairs; the repeaters are responsible for replenishing their supply of shorter-distance pairs in order to make the end-to-end Bell pairs.

In teleportation, the state of a qubit is destroyed in one location and recreated in another. First, a Bell pair is distributed, with one member held at the source (Alice) and the other at the destination (Bob). The qubit to be teleported (which we will call the data qubit) is entangled with Alice's member of the Bell pair. Then both the data qubit and Alice's Bell qubit are measured. Each measurement results in one classical bit, and destroys the quantum state of the qubit. The two classical measurement results are communicated to Bob, who then uses them to decide what quantum operations on his Bell qubit will recreate the original state of the data qubit.

The original creation of the Bell pair must begin with a quantum operation that entangles two distant qubits, as described in Section II-A, but the teleportation operation itself requires only local quantum operations and classical communication between Alice and Bob.

In a system of quantum repeaters, the use of teleportation moves the state of a single qubit from one station to another. If the qubit being teleported is a member of (another) Bell pair, that relationship is preserved, but one of the end points moves. Figure 2(a) illustrates this process, known as *entanglement swapping*. A Bell pair spanning nodes 0 and 1 ($0 \leftrightarrow 1$) and a pair spanning nodes 1 and 2 ($1 \leftrightarrow 2$) are used to create a single $0 \leftrightarrow 2$ pair. The qubit in Station 1 in step 1 is teleported to Station 2, lengthening the distance between the end points of the black Bell pair. Step 1 is the creation of the base-level Bell pairs. Step 2 is local quantum operations at the middle node, including the measurement of both qubits, followed by classical communication to the end nodes, then possibly local operations at the destination node to complete the recreation of the teleported qubit. This teleportation destroys the right-hand Bell pair, and frees the two qubits in the middle for reuse.

In theory, any three nodes with two Bell pairs can use entanglement swapping, but most designs presented to date assume that a chain of repeaters will double the distance between end points of the Bell pair each time swapping is performed, combining two n-hop Bell pairs into one $2n$-hop pair. Briegel *et al.* [21] established the use of such a doubling architecture in early discussions of quantum repeaters, and showed that performance declines polynomially rather than exponentially with distance [3]. If purification always succeeds, this logarithmic-depth combination of links intuitively appears to be optimal, though we know of no proof of this hypothesis. Jiang *et al.* have begun investigating relaxing that constraint dynamically, allowing neighboring Bell links of any length to combine [49]. This approach is promising for probabilistic systems, and necessary when physical constraints dictate that the number of hops is not a power of two.

In the simulations presented here, we assume the use of a basic doubling architecture for swapping. We call the number of times swapping has been performed the “level” of the Bell pair, with level 0 being our base Bell pairs at a distance of one hop. A Bell pair of level i spans 2^i hops. Figure 2(b) shows three levels of Bell pairs, representing the state after zero, one, and two levels of swapping. In the end, one pair has been stretched to reach four hops, and the other three Bell pairs present at level 0 have been destroyed and the physical qubits freed for reuse.

III. Quantum Repeater Protocol Stack

To give an overview of the processing and message flow in a repeater network, Section II discussed repeater behavior as an integrated phenomenon. However, the actions can be cleanly separated into a layered protocol stack, as shown in Figure 3(a). The bottom, *physical entanglement* (PE) layer corresponds to the wavy lines in Figure 1, using strong laser pulses or single photons to create the shared quantum state between two distant qubits. The next layer, *entanglement control* (EC), consists primarily of the “keep” flags indicating the success or failure of entanglement attempts. These bottom two layers operate only across a single hop. Above these layers reside the *purification control* (PC) and *entanglement swapping control* (ESC) layers. PC consists of a series of messages indicating the pairs on which purification was attempted, and the results. PC must operate at each power of two distance, 1 to 2^n, for a 2^n-hop link. Figure 1 shows the messaging sequence for PE, EC, and the lowest layer of PC.

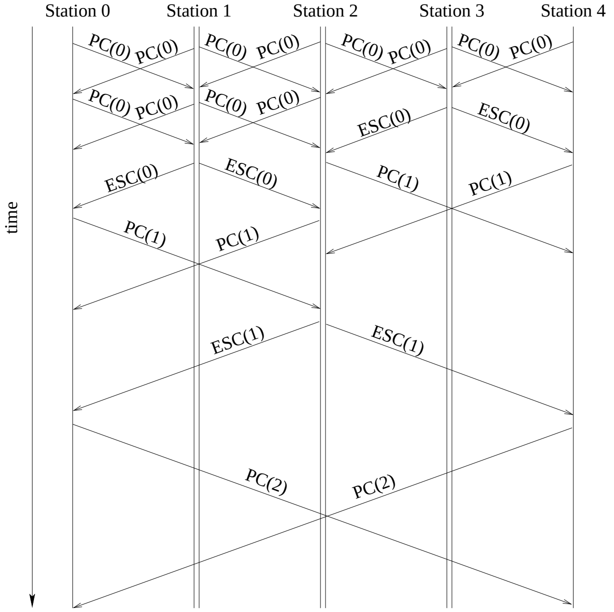

Fig. 4. Example message sequence for purification control (PC) and entanglement swapping control (ESC). Numbers in parentheses are the level, or distance.

ESC, which supports the teleportation that splices two Bell pairs to create one pair that spans a greater distance, must involve three nodes, as shown in Figure 2 and described in Section II-C. ESC must inform one of its partners (generally, the one on the right in the diagram, as we assume qubits are being teleported left to right) of the results of its local operations, which are probabilistic. The right-hand node may need to perform local operations based on the results received. The left-hand node must also be informed of the basic fact of the swapping operation. ESC at the middle station unconditionally returns the qubits just measured to PE for reuse. The left and right stations pass control of their qubits to the PC level above the current ESC, for purification at the new distance.

In normal operation, purification and swapping (PC and ESC) are repeated at each level until the top, end-to-end level is reached, as shown in Figures 3(b) and 4. At that final distance, purification (PC) may be repeated one more time to create the final end-to-end pair of the fidelity required by the application. Of course, purification can be omitted or repeated at any level, depending on the fidelity of the Bell pairs. In Figure 4, purification at level 0 is shown happening twice on the left. The actual timing of messages may vary somewhat; PC(0) can only be initiated after the status of qubits has been established by EC, as in Figure 1. Because the stations run

[3] Portions of their analysis apply to the splicing of more than two links in each swapping step, but they always discuss a regular, exponential growth in the span of Bell pairs, and their most detailed analysis uses the doubling approach.

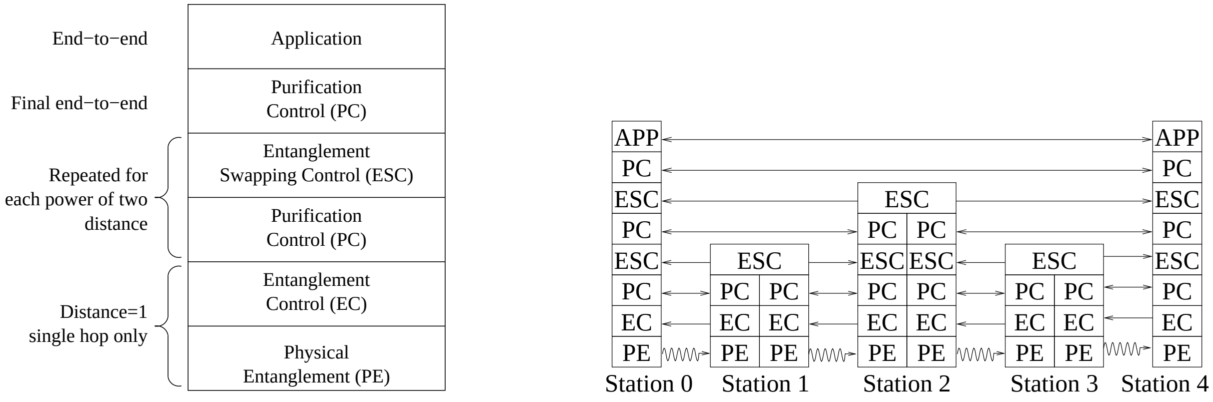
End−to−end
Application
Final end−to−end
Purification Control (PC)
Repeated for each power of two distance
Entanglement Swapping Control (ESC)
Purification Control (PC)
Distance=1 single hop only
Entanglement Control (EC)
Physical Entanglement (PE)
APP
PC
ESC
EC
PE
Station 0
Station 1
Station 2
Station 3
Station 4

(a) protocol stack

(b) layer interactions

Fig. 3. Protocol stack and layer interactions for quantum repeater operation.

a deterministic algorithm to select which pairs to purify, PC does not need to negotiate which operations to perform, only inform its partner of the outcomes.

When the network is a single line of $N = 2^n$ hops, each station can easily determine the other stations to which it must build PC and ESC connections. In a network with a richer topology, this process must involve routing for the end-to-end connection. The middle meeting point of each entanglement swapping level must be identified. Some form of source routing or circuit setup will be required, especially when the number of hops is not a power of two; we defer this problem to future work.

Both the stations themselves and the qubits they hold must be addressable. Because PC and ESC can involve any stations, the control protocols must be designed to include general station addresses. EC, PC, and ESC must also be able to address qubits at both ends of each connection and to share those addresses with other nodes and protocol layers. The addresses can be logical, and a station may relocate its half of any Bell pair from one internal qubit to another without notifying its partners, provided it can continue to match incoming and outgoing messages to the correct qubits. Once the base Bell pair is created, the qubits no longer need a direct connection to the long distance quantum communication channel.

IV. Purification Scheduling

Section II-B deferred discussion of a critical point: two stations trying to take a set of lower-fidelity pairs and create a higher-fidelity pair must decide which pairs to purify. The algorithm used determines the physical resources required and the speed of the convergence to the target fidelity. Our new banded purification scheduling algorithm raises the throughput of a given hardware configuration by a factor of up to fifty, and provides greater flexibility in hardware configuration. Before we present banding, we describe the *symmetric* and *pumping* scheduling algorithms, then our prior greedy algorithm.

Symmetric purification, described by Dür *et al.* as schemes A and B [48], requires pairs to attempt to purify only with other pairs of the same fidelity. Figure 5a shows the evolution and history of a symmetrically-grown Bell pair. In the figure, for simplicity, base-level Bell pairs are created in odd-numbered time steps, and purification operations are attempted in even-numbered time steps. (The fidelities in the diagrams in this section are for illustration only, and are not exact.) At $t = 4$, the symmetric algorithm would not attempt to purify the fidelity 0.71 pair with the fidelity 0.638 pair, instead waiting for the development of a second fidelity 0.71 pair at $t = 6$.

Symmetric purification would take our starting fidelity of 0.638 to e.g. a target fidelity of 0.98 after five rounds. If purification always succeeded, thirty-two (2^5) base-level Bell pairs would be required: $32 \times 0.638 \rightarrow 16 \times 0.71 \rightarrow 8 \times 0.797 \rightarrow 4 \times 0.867 \rightarrow 2 \times 0.952 \rightarrow 1 \times 0.988$. Unfortunately, purification is a state-dependent, probabilistic operation. When using our starting state, the first step (0.638 + 0.638) will succeed only 57% of the time, while the last step will succeed 92% of the time. In total, symmetric purification actually consumes, on average, more than 450 base-level Bell pairs to make one Bell pair of 0.98 fidelity.

The principal drawbacks to the symmetric algorithm are the inflexible use of available resources, both time and space (as shown by e.g. the wait at $t = 4$ in the figure), and the fact that the truly symmetric history tree is effectively impossible to achieve. Memory degradation over time causes two pairs that arrived at different times to have different fidelities, so forcing exact matches only is impractical.

Entanglement pumping, defined by Dür *et al.* as Scheme C and shown in Figure 5b, can be done using only the minimum two qubits in each station [22]. The fidelity of one Bell pair is pumped by purifying with base-level pairs created using the physical entanglement mechanism. This scheme uses physical resources efficiently, but improves the fidelity of entanglement only slowly; when the fidelity difference between the base pairs and the final target fidelity is large, pumping is ineffective.

Previous work [25] considered a greedy scheduling algorithm for purification scheduling: at each time step, all available resources are purified, never deferring immediate

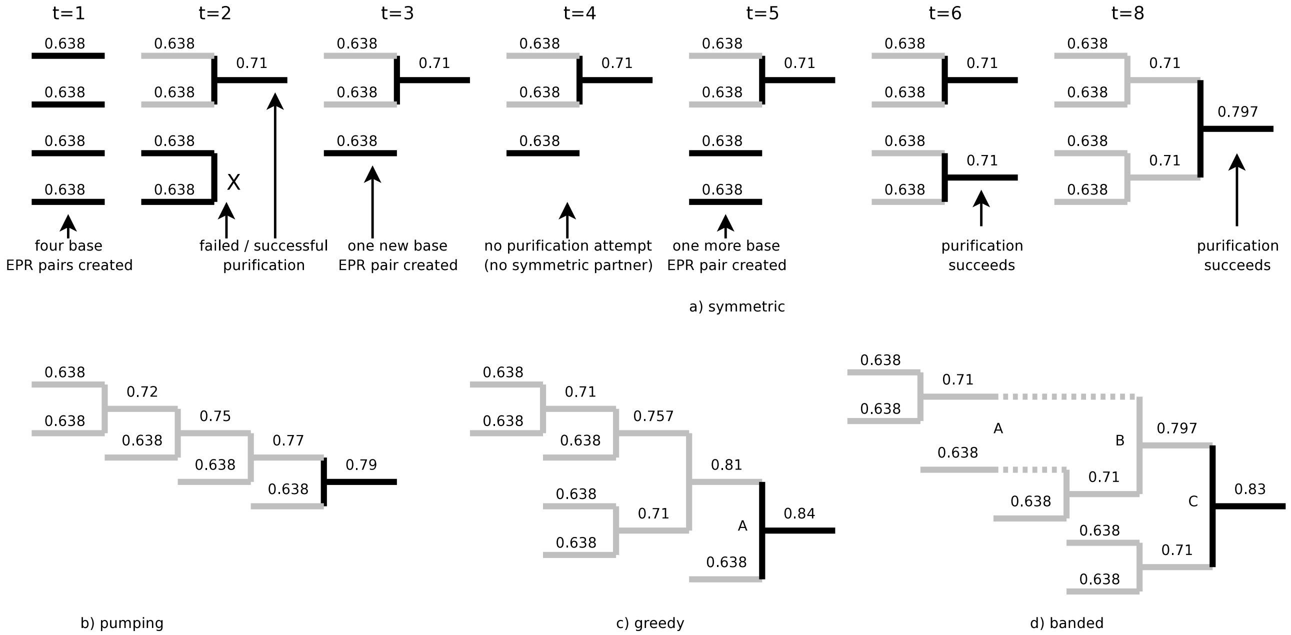
t=1
t=2
t=3
t=4
t=5
t=6
t=8
0.638
0.71
0.797
X
four base EPR pairs created
failed / successful purification
one new base EPR pair created
no purification attempt (no symmetric partner)
one more base EPR pair created
purification succeeds
purification succeeds
0.72
0.75
0.77
0.79
0.757
0.81
0.84
A
B
C
0.83

a) symmetric

b) pumping

c) greedy

d) banded

Fig. 5. Different purification scheduling algorithms. Gray bars represent the *history* of the pair. Black horizontal bars represent currently entangled Bell pairs. Numbers show the fidelity of the Bell pair. a) Logical evolution of a symmetrically-grown Bell pair. b) History tree of a Bell pair grown using the entanglement pumping algorithm. c) History tree of a Bell pair grown using the greedy algorithm. d) An example history of the evolution of a Bell pair using our new banded purification algorithm. If the boundary between two bands is placed at e.g. 0.66, at point A, the pairs 0.71 and 0.638 will not be allowed to purify. Dashed lines represent time that Bell pairs are forced to wait for a suitable partner to be created.

actions in favor of potential later operations. Figure 5c shows one possible history tree. When the fidelity of a base Bell pair is high, above ~ 0.75 or so, this scheme works well. However, when the fidelity is lower, because of longer distances or loss elsewhere in the system, a greedy algorithm results in attempts to purify a high-fidelity pair with a low-fidelity pair, as at the point A in the figure. Using a low-fidelity pair both has a lower probability of success and gives only a small boost in fidelity when it succeeds. Thus, the effective floor for the fidelity of base pairs when using the greedy algorithm is high.

We have seen that the greedy algorithm and entanglement pumping sometimes match Bell pairs with very different fidelities, resulting in low probability of success for the purification operation and giving only a limited boost in fidelity even on success. The fully symmetric tree is impractical: it imposes strict minimum hardware requirements, cannot allocate resources flexibly, and in practice cannot take into account memory degradation. A new approach is required.

We have developed *banded* purification to match purification pairs efficiently but flexibly. We divide the fidelity space into several regions, or bands, and only allow Bell pairs within the same band to purify with each other. Figure 5d shows a simple example, assuming two bands divided at a fidelity of 0.66. At the point A, the greedy algorithm would attempt to purify the 0.638 pair with the 0.71 pair (as shown at A in Figure 5c). When using banding, the band boundary at 0.66 prevents those pairs from purifying, and so the system waits for the creation of another fidelity 0.638 pair, then purifies the two 0.638 pairs. If that purification is successful, resulting in a second 0.71 pair, then purification will be attempted at point B using the two 0.71 pairs. At point C, the banding structure allows the new 0.71 pair to purify with the 0.797 pair, whereas the symmetric algorithm would block temporarily. Unlike the greedy and pumping algorithms, the banded approach treats high-fidelity pairs as more valuable than low-fidelity pairs, and only uses them when another similarly high pair is available, making those operations more likely to succeed and providing a larger boost in fidelity.

Recall that the purification operations can fail, but their probability of success increases as the fidelity of the pairs involved increases. Any attempt to predict the exact best sequence of purification operations from a given state, therefore, must take into account which resources are currently busy, the fidelities of all available Bell pairs, the probability of success of possible purification choices, and the probability that currently unentangled qubits will be successfully entangled in the near future using the physical entanglement mechanism.

The banded and symmetric algorithms are potentially subject to deadlock, but the problem is easily solved for the banded algorithm. If a repeater has e.g. seven qubits and seven bands (or seven rounds of purification for the symmetric case), one Bell pair could be in each band. Each pair would have no possible purification partner, and no free qubits would be available to create new pairs to add to the bottom band. Each swapping level is independent, so the minimum number of qubits per station must actually be the number of bands times the number of levels, plus one, for the receive half and send half of the repeater. In our simulations, we select a hardware configuration, then restrict the number of bands used to a number that will not deadlock. The symmetric algorithm has no such flexibility.

V. Simulation Results

We have simulated repeater chains for a broad range of the parameters discussed in prior sections. The majority of our simulations utilize banded purification, and the greedy algorithm is simulated for comparison. We simulate the quantum mechanics of the physical interactions and operations, but a large fraction of the code (7,000 lines of C++) and execution time (several weeks on eight 3.0GHz+ Intel processors) are dedicated to managing the messages that are transferred station to station.

The metric we use to evaluate quantum networks is the throughput, measured in Bell pairs per second of a certain fidelity over a given distance. We have chosen a target fidelity of 0.98, and simulate for distances up to 20,000 kilometers. Unless otherwise specified, the simulations presented here are for 64 links of 20 kilometers each with one hundred qubits per station (50 for receive and 50 for send, except at the end points where all 100 can be used for one direction). Our simulations all assume 0.17 dB/km loss and a signal propagation speed of $0.7c$, corresponding to telecommunications fiber. In the hybrid quantum repeater schemes we simulate, fiber loss translates to reduced fidelity for a Bell pair, rather than a lower success rate [24], [25]. For 20km links at $0.7c$, the one-way latency for signals is just under 100μsec, so the "clock rate" for these simulations is about 10kHz. As noted above, the pulses are very short compared to the propagation latency, and for the settings we use, entanglement is successful about forty percent of the time. With these settings, in the first time step, each station will attempt to entangle fifty qubits, successfully creating about twenty base-level Bell pairs on each link. In successive time steps, the number of attempts on each link is capped by the number of available qubits at each station.

Our code is capable of simulating imperfect local gates, but to isolate the individual factors presented here, the simulations in this paper assume perfect local quantum operations and memory. Our simulations have shown that gate errors of 0.1% result in about a factor of two reduction in the performance of the system, with performance degrading rapidly and a final fidelity of 0.98 being unattainable with gate errors of 0.3%. A complete discussion of error mechanisms in quantum computing and the current experimental state of the art is beyond the scope of this paper, but this level of quality is well beyond what is currently possible; the number 0.1% should be viewed as a *target* which experimentalists should strive to achieve.

As a rough approximation, the gate error rate can be considered to be the *combination* of both local gate errors and memory errors. With one-way latency in fiber of approximately 6msec at 1,280km, memory must be able to retain its state for times on the order of seconds to meet the above constraint. Hartmann *et al.* have recently examined the role of memory errors in quantum repeaters [23], finding that memory that can successfully retain a quantum state for about one second can support ultimate repeater distances of 5-20,000km, albeit it at large cost in resources and with a cap on the achievable fidelity. If memory times are substantially shorter, then local quantum error correction should be added, which will add substantial additional complexity to the system design.

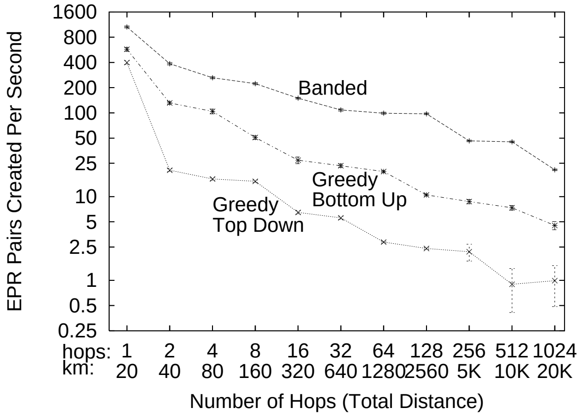

Fig. 6. Throughput versus distance for the banded algorithm using five bands, compared to the greedy bottom up and greedy top down algorithms. The final fidelity is 0.98.

For each banded data point in the graphs presented here, extensive runs over large parameter spaces (up to 800 or so separate sets of parameter settings) were executed to find a good set of bands, and to find a good set of thresholds for entanglement swapping at different distances. Each data point represents a single run in which 200 end-to-end Bell pairs of final fidelity 0.98 or better are created, with the exception of a few of the slowest data points, which were terminated early. The throughput is calculated by linear regression to fit a line to the arrival times of the Bell pairs [50]. Error bars are included for all graphs except Figure 7 but are almost too small to be seen at many data points; they represent the standard deviation of the fitted slope for that run. The coefficient of determination is above 0.996 for almost every fit except the three data points with the largest error bars in Figure 6, for which it is 0.95, 0.80, and 0.78. These fits confirm that despite the stochastic nature of the quantum operations, the mean arrival rate is constant after the initial transient startup latency. Runs of fewer than 200 Bell pairs were found to have unacceptably large variability. Data, log files, and parameter settings for all runs are available from the authors.

First we analyze the performance of the greedy algorithm, then present our primary results, comparing the throughput of greedy and banded purification. We backtrack to explain how bands are selected, then compare several options for setting the fidelity target at each swapping level. The final two subsections explore the hardware configuration, assessing the importance of the number of qubits per station and the trade-off of distance versus repeater size.

A. Greedy Algorithm

The performance of the greedy top down algorithm, corresponding to our prior work, is the bottom line in Figure 6 [25].

Throughput in end-to-end Bell pairs created per second is plotted against distance. The X axis is labeled with both the number of hops and total distance in kilometers; the rightmost point of 1,024 hops or 20,000 kilometers corresponds roughly to the distance halfway around the world.

For the greedy top down algorithm, throughput is about 21 Bell pairs/second for two hops, and declines to almost exactly 1 Bell pair/second for 1,024 hops. The decline shows a distinct stair-step structure, caused by the discrete nature of purification and our choice to purify until a final fidelity of 0.98 is reached. At a particular length, a certain number of purification steps is required to achieve the final fidelity. As the number of hops increases, the same number of purification steps may continue to serve, until the fidelity drops below the target and an additional round of purification must be added. When this happens, the performance drops by roughly a factor of two, as two high-quality pairs up near the target are required.

The greedy algorithm sorts the Bell pairs by fidelity, and pairs them starting with the two highest-fidelity pairs. We discovered that pairing beginning from the bottom of the list, which we term greedy bottom up, increases performance by a factor of three to eight, as the middle curve in Figure 6 shows. We attribute this improvement to increased conservatism on the use of the highest-fidelity pair. Beginning at the bottom will bring other pairs up toward the fidelity of the highest pair, perhaps even surpassing it, but first risking the failure of lower-fidelity pairs which have cost less to build.

At the left hand edge of the graph, the greedy top down algorithm declines from 400 pairs/second for one hop to 21 for two hops, almost a factor of twenty worse. For this graph, our hardware is assumed to have one hundred qubits per station. For one hop, all one hundred qubits can directly connect to qubits at the far end. For two hops, the middle station must split the use of its one hundred qubits, fifty for the left-hand link and fifty for the right-hand link. The difference is due to more efficient purification pairings as the number of available qubits grows. This effect is assessed in more detail in Section V-E.

B. Banded Performance v. Total Distance

The top line in Figure 6 graphs the performance of our banded algorithm. Throughput starts at 1060 Bell pairs/second for one hop, plateaus at about 100 for 32 to 128 hops, then declines to 20 pairs/second for 1,024 hops. Due to the stair-step behavior, the benefit compared to the greedy top down algorithm varies from a factor of fifteen to a factor of fifty, with the advantage growing unevenly as distance increases. Compared to the greedy bottom up algorithm, banded is 2.5 to 9.3 times better, also increasing unevenly with distance.

Entanglement pumpting and symmetric scheduling are not shown in the figure. Entanglement pumping cannot effectively create pairs of fidelity 0.98 with our starting fidelity of 0.638. For the particular configuration shown here, the symmetric algorithm would perform similarly to banding. However, as noted in Section IV, the fully symmetric algorithm cannot be achieved in practice.

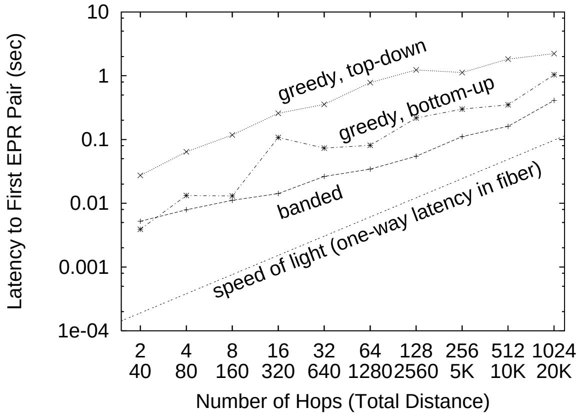

Fig. 7. Startup latency versus distance for the banded, greedy bottom up, and greedy top down algorithms.

An important question is whether band structure changes when the total distance (number of hops) is increased. If the band structure does not change, then we can simulate short lines, and apply the simulation results directly to much longer lines, dramatically reducing the amount of computation time needed in simulations. Likewise, in real-world operational environments, distance-independent system controls would be a boon. Unfortunately, our simulations have shown that the banding structure does vary somewhat at different distances. The performance for nearby banding structures can be a factor of two worse, meaning that a careful search is necessary for each specific link configuration.

Because the Bell pairs created are a generic resource that do not initially carry application data, the normal operation mode for the system will be steady-state, continuous operation, buffering prepared Bell pairs to the extent possible during times when applications are not consuming them. As noted in Section I, the distributed nature of repeater operations means that there is no true “in flight” time for a qubit. Nevertheless, a quick look at the latency to start up the system is in order. Figure 7 shows the latency from the time the system is started until the first end-to-end Bell pair is created. The values graphed are the latency for the first Bell pair for each of the runs in Figure 6. For the banded algorithm, start-up latency is about fifteen times the one-way latency for two hops, declining to about four times the latency for 1,024 hops.

C. Finding the Bands

We can theoretically place the boundaries that separate bands at almost any level. To determine a placement that gives good performance, we have performed nearly exhaustive searches over many possibilities, for configurations with two to six bands. Figure 8 shows a two-band setup. In this figure, we vary the boundary in steps of 0.01, but in most other graphs the steps are 0.02 or 0.04. At the left edge, the division between the two bands is below the initial threshold of 0.638 generated by our physical entanglement process, and at the right edge the division is above the delivery threshold for our

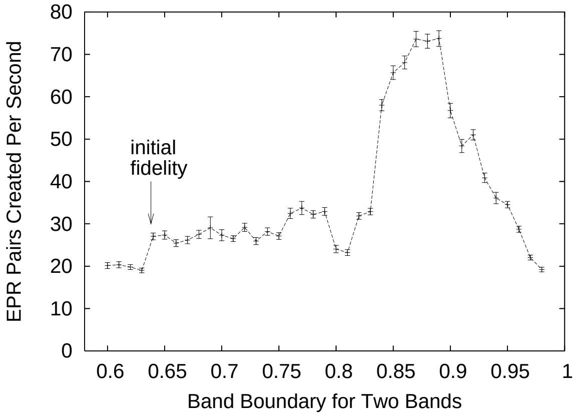

Fig. 8. Finding the best band boundary for a 2-band arrangement, for 64 hops of 20km each.

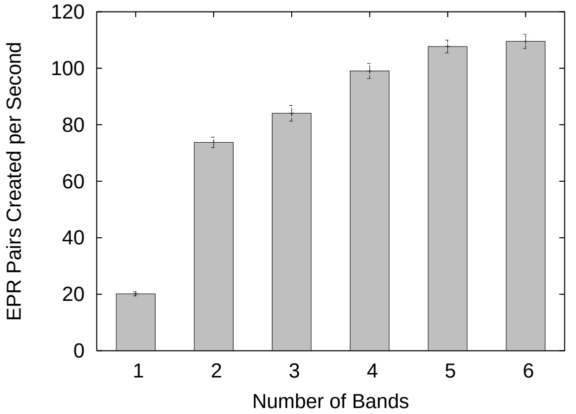

Fig. 9. The best band throughput for different numbers of bands, for 64 hops of 20km each.

final qubits, resulting in the equivalent of the bottom up greedy algorithm for the first and last data points. The performance peaks when the band boundary is 0.87-0.89, showing clearly that the operational imperative is protecting the high-fidelity pairs from purifying with low-fidelity pairs.

Increasing the number of bands gives a smooth increase in performance for up to five bands, which perform nearly 50% better than two bands. Figure 9 shows the increase in performance for increasing numbers of bands. Moving from one band (equivalent to greedy bottom up) to two increases performance by more than a factor of three. The performance has saturated with six bands; it is not clearly better than five bands, because the behavior has essentially been constrained to that of a symmetric tree. For more than two bands, the number of simulation runs to cover the space increases geometrically, so the granularity of our boundary steps is somewhat larger. For three bands, for example, we tried all combinations of boundaries with the lower bound varying 0.60 to 0.95, and the upper boundary varying from 0.80 to 0.99, in steps of 0.02.

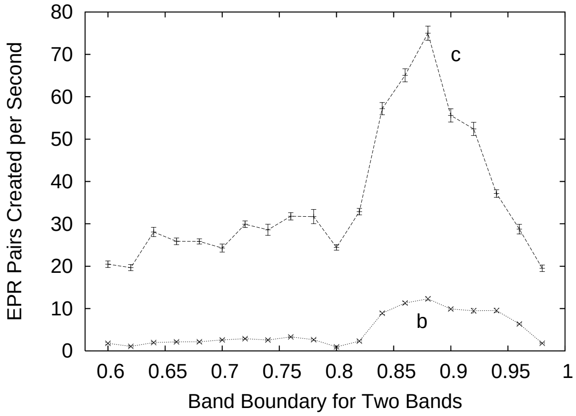

Fig. 10. Comparing different distance-swapping thresholds.

D. Varying Swapping Thresholds

Recall the distinction between the purification bands and thresholds at different distances: the former governs purification decisions within PC, while the latter governs the promotion of pairs from PC to ESC for entanglement swapping at the next-higher distance. The experiments in the previous subsections were performed with each of the distance thresholds set to 0.98. In this section, we evaluate several possible sets of thresholds that seem like plausible candidates for good configurations:

a. 0.9, 0.9, 0.9, 0.9, 0.9, 0.9, 0.98:
purify only to an intermediate fidelity of 0.9 at distance 1, 2, 4, 8, 16, and 32, then push to the final fidelity of 0.98 at the full distance of 64 hops;

b. 0.98, 0.9, 0.9, 0.9, 0.9, 0.9, 0.98:
purify to fidelity 0.98 at distance 1, then allow the fidelity to slip as far as 0.9 at intermediate distances, before pushing back up to 0.98 at 64 hops; and

c. 0.98, 0.98, 0.98, 0.98, 0.98, 0.98, 0.98:
purify to fidelity 0.98 at distance 1, then maintain that fidelity by purifying as necessary at each distance.

Figure 10 shows clearly that the preferred method of managing the fidelity of a pair as it hops across the network is case **c**, purifying to the desired level at distance one, and maintaining that fidelity at all distances. Case **a** proved to perform so poorly that the simulations were unable to complete. The other two cases are shown in the figure.

This data supports the intuitive idea that purifying over short distances will be more efficient than purifying over long distances. Dür *et al.* referred to this approach as maintaining a “working fidelity” [48]. They did not report on any alternative schemes, but our data confirms that their approach is correct.

In addition, we investigated several other candidate schemes, all of which performed worse than maintaining a working fidelity; those results confirm our findings presented here.

Because the curves for **b** and **c** have the same shape, despite radically different distance thresholds, Figure 10 also suggests that changing the pattern of fidelity thresholds at

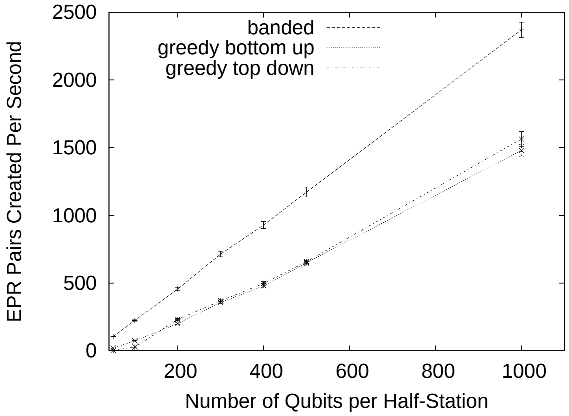

Fig. 11. Comparing different numbers of qubits per station, for five bands, greedy bottom up, and greedy top down. Simulations are 64 hops of 20km each.

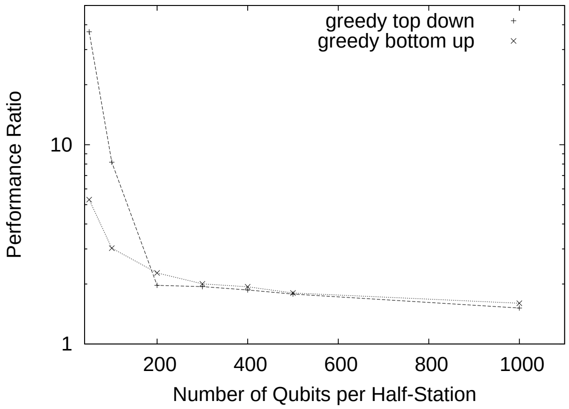

Fig. 12. Performance ratio of banded purification compared to the two forms of greedy purification, bottom up and top down.

different distances is *independent* of the choice of the bands for banded purification. That is, a good choice of bands should remain good regardless of the thresholds at various distances. This fact should allow us to optimize these two parameters independently for a given physical configuration.

E. Number of Qubits per Station

The principal constraint on throughput is the number of qubits per station. What will happen as our hardware capabilities grow? How should we distribute limited physical resources? This subsection and the next address these two important questions.

The throughput achieved for two bands with varying numbers of qubits per half-station is shown in Figure 11. The throughput achievable with five-band purification scheduling is linear in the number of qubits.

Banding is especially valuable in the near term, when station capacities are expected to be one of the principal engineering constraints. The greedy top down algorithm performs poorly with small numbers of qubits per station. With larger numbers of qubits in various stages of development, simply ordering the list and partnering Bell pairs bottom up will naturally tend to use qubits that are of similar fidelity, giving similar behavior to banding without a formal band structure. Figure 12 shows this effect, with the banded algorithm outperforming the greedy algorithms at all station sizes, but by a smaller ratio as the station capacity grows. With 50 qubits per half-station, the greedy top down algorithm struggles to meet our fidelity goal of 0.98, and banded performs thirty-seven times better.

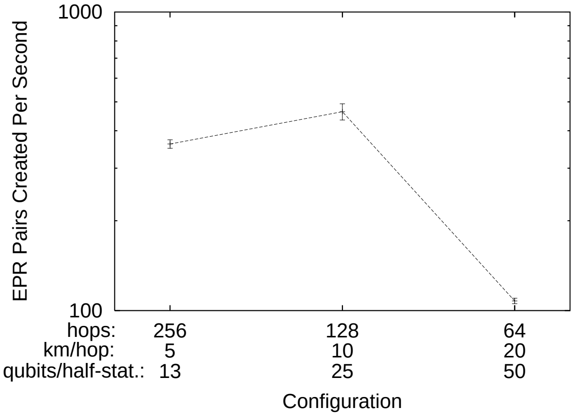

Fig. 13. Best throughput for about 6,500 qubits spread over 1,280km.

F. Varying Number of Stations

Because physical qubits may be the scarce resource in a repeater system, it makes sense to ask how best to spread the qubits out along a link to achieve the maximum throughput. With the exception of Section V-E, most of the experiments presented so far in this paper have used 64 hops of 20km each with 50 qubits per half-station, but what if we were to split each repeater and create 128 hops of 10km with 25 qubits per half-station, or 256 hops of 5km with 13 qubits? These three cases are shown in Figure 13. As the number of qubits per half-station decreases, we must restrict the number of bands in order to avoid deadlock. For 64 hops and 50 qubits, we can use five bands; for 128 hops and 25 qubits, only three; and for 256 hops with 13 qubits only a single band. This fact gives us an engineering trade-off; bands are especially useful in lower-fidelity hops, helping to offset the decrease in throughput that comes from lengthening the hops.

This section has shown some preliminary explorations of this question, but the space of possibilities is large, and for both long and short hops, additional factors such as memory errors and local gate errors will likely play larger roles. A more complete analysis would require a combinatorial increase in the number of simulations performed; the total simulation time of more than half a CPU-year would be multiplied by the number of swapping thresholds tested for each of seven thresholds in the configurations above. We defer more a complete analysis to future work.

VI. Conclusion

The banded purification algorithm and hardware parameters presented here represent a step forward in quantum repeater network design, as shown by the gains in throughput we report, especially with intermediate numbers of qubits per station. Banded purification provides throughput essentially identical to fully symmetric purification. Symmetric purification, however, cannot be achieved in practical systems, due to memory degradation and the possibility of deadlock. These gains are more than hypothetical; the improved operation at low initial fidelities will assist the first laboratory experiments of a complete repeater network, which inevitably will operate at the very edge of a functional system. Although the basic concepts of quantum repeaters are simple, physical realizations remain some years away. The dynamic behavior is analytically intractable and the range of engineering parameters broad, making simulation a valuable tool. Our simulations have helped us to identify important hardware constraints and test possible protocols, allowing us to find improvements that raise performance by a factor of fifteen to fifty across a broad range of distances and parameters, and to extend the possible operating range to lower fidelities (down to a fidelity of below 0.55, compared to greater than 0.7 for prior simulations).

We have laid out a rudimentary architecture for the protocols necessary to operate a network of repeaters. We know that buffer qubits must have addresses at the entanglement control (EC) level and above. At the purification control (PC) level and above, stations must also have addresses. These addresses must be shareable across layers of the protocol stack. Software-selectable characteristics of the protocols, such as bands and thresholds for promotion to longer swap distances may be locally-held information only, decided out of band, or dynamically negotiated through an additional session control protocol; we defer such design issues until experimental progress demands.

Banded purification will be useful for quantum system-area networks (SANs), as well as wide-area quantum networks. In wide-area quantum networks, loss is dominated by the length of the fiber. In SANs for quantum multicomputers [13], [51], fiber losses will be low, but losses elsewhere in the system (e.g., the qubit-fiber coupling or node-to-node switching) will be present, requiring the use of purification. Our results will assist the development of distributed quantum computing systems with node-to-node distances ranging from a handspan to intercontinental, helping to usher in the era of quantum computation.

Acknowledgments

The authors thank NICT for partial support for this research. We thank Kohei M. Itoh, Peter van Loock, John Heidemann and Joe Touch for valuable discussions.

References

[1] Lieven M. K. Vandersypen, Matthias Steffen, Gregory Breyta, Constantino S. Yannoni, Mark H. Sherwood, and Isaac L. Chuang. Experimental realization of Shor's quantum factoring algorithm using nuclear magnetic resonance. *Nature*, 414:883–887, December 2001.

[2] Stephan Gulde, Mark Riebe, Gavin P. T. Lancaster, Christoph Becher, Jurgen Eschner, Hartmut Haffner, Ferdinand Schmidt-Kaler, Isaac L. Chuang, and Rainer Blatt. Implementation of the Deutsch-Jozsa algorithm on an ion-trap quantum computer. *Nature*, 421:48–50, 2003.

[3] Michael A. Nielsen and Isaac L. Chuang. *Quantum Computation and Quantum Information*. Cambridge University Press, 2000.

[4] Peter W. Shor. Algorithms for quantum computation: Discrete logarithms and factoring. In *Proc. 35th Symposium on Foundations of Computer Science*, pages 124–134, Los Alamitos, CA, 1994. IEEE Computer Society Press.

[5] Daniel S. Abrams and Seth Lloyd. Quantum algorithm providing exponential speed increase for finding eigenvalues and eigenvectors. *Physical Review Letters*, 83:5162–5165, 1999.

[6] Rodney Van Meter and Mark Oskin. Architectural implications of quantum computing technologies. *ACM Journal of Emerging Technologies in Computing Systems*, 2(1):31–63, January 2006.

[7] Pieter Kok, W. J. Munro, Kae Nemoto, T. C. Ralph, Jonathan P. Dowling, and G. J. Milburn. Review article: Linear optical quantum computing. *Reviews of Modern Physics*, 79:135, 2007.

[8] C. Negrevergne, T.S. Mahesh, C.A. Ryan, M. Ditty, F. Cyr-Racine, W. Power, N. Boulant, T. Havel, D.G. Cory, and R. Laflamme. Benchmarking quantum control methods on a 12-qubit system. *Physical Review Letters*, 96:170501, 2006.

[9] H. Häffner, W. Hänsel, C. F. Roos, J. Benhelm, D. Chek al kar, M. Chwalla, T. Körber, U. D. Rapol, M. Riebe, P. O. Schmidt, C. Becher, O. Gühne, W. Dür, and R. Blatt. Scalable multiparticle entanglement of trapped ions. *Nature*, 438:643–646, 2005.

[10] Lov K. Grover. Quantum telecomputation. http://arXiv.org/quant-ph/9704012, April 1997.

[11] R. Cleve and H. Buhrman. Substituting quantum entanglement for communication. *Physical Review A*, 56(2):1201–1204, 1997.

[12] J.I. Cirac, A. Ekert, S.F. Huelga, and C. Macchiavello. Distributed quantum computation over noisy channels. *Physical Review A*, 59:4249, 1999.

[13] Rodney Van Meter, W. J. Munro, Kae Nemoto, and Kohei M. Itoh. Arithmetic on a distributed-memory quantum multicomputer. *ACM Journal of Emerging Technologies in Computing Systems*, 3(4):17, January 2008. available as arXiv:quant-ph/0607160v2.

[14] Jeffrey Yepez. Type-II quantum computers. *International Journal of Modern Physics C*, 12(9):1273–1284, 2001.

[15] S. Lloyd, M. S. Shahriar, and P.R. Hemmer. Teleportation and the quantum Internet, 2000. http://arXiv.org/quant-ph/0003147.

[16] C. H. Bennett and G. Brassard. Quantum cryptography: Public key distribution and coin tossing. In *Proc. IEEE International Conference on Computers, Systems, and Signal Processing*, pages 175–179. IEEE, December 1984.

[17] Kenneth G. Paterson, Fred Piper, and Ruediger Schack. Why quantum cryptography? http://arxiv.org/quant-ph/0406147, June 2004.

[18] Chip Elliott, David Pearson, and Gregory Troxel. Quantum cryptography in practice. In *Proc. SIGCOMM 2003*. ACM, ACM, August 2003.

[19] Yoshihiro Nambu, Ken'ichiro Yoshino, and Akihisa Tomita. One-way quantum key distribution system based on planar lightwave circuits. *Japanese Journal of Applied Physics*, 45:5344, 2006.

[20] Romain Alleaume, Jan Bouda, Cyril Branciard, Thierry Debuisschert, Mehrdad Dianati, Nicolas Gisin, Mark Godfrey, Philippe Grangier, Thomas Langer, Anthony Leverrier, Norbert Lutkenhaus, Philippe Painchault, Momtchil Peev, Andreas Poppe, Thomas Pornin, John Rarity, Renato Renner, Gregoire Ribordy, Michel Riguidel, Louis Salvail, Andrew Shields, Harald Weinfurter, and Anton Zeilinger. SECOQC white paper on quantum key distribution and cryptography. quant-ph/0701168, January 2007.

[21] H.-J. Briegel, W. Dür, J.I. Cirac, and P. Zoller. Quantum repeaters: the role of imperfect local operations in quantum communication. *Physical Review Letters*, 81:5932–5935, 1998.

[22] L. Childress, J.M. Taylor, A.S. Sørensen, and M.D. Lukin. Fault-tolerant quantum repeaters with minimal physical resources and implementations based on single-photon emitters. *Physical Review A*, 72(5):52330, 2005.

[23] L. Hartmann, B. Kraus, H.-J. Briegel, and W. Dür. On the role of memory errors in quantum repeaters. *Physical Review A*, 75:032310, 2007.

[24] P. van Loock, T. D. Ladd, K. Sanaka, F. Yamaguchi, Kae Nemoto, W. J. Munro, and Y. Yamamoto. Hybrid quantum repeater using bright coherent light. *Physical Review Letters*, 96:240501, 2006.

[25] T.D. Ladd, P. van Loock, K. Nemoto, W. J. Munro, and Y. Yamamoto. Hybrid quantum repeater based on dispersive CQED interaction between matter qubits and bright coherent light. *New Journal of Physics*, 8:184, 2006.

[26] T. Yamamoto, M. Koashi, S.K. Ozdemir, and N. Imoto. Experimental

extraction of an entangled photon pair from two identically decohered pairs. *Nature*, 421(6921):343–6, 2003.

[27] W. K. Wootters and W. H. Zurek. A single quantum cannot be cloned. *Nature*, 299:802, October 1982.

[28] C. H. Bennett, G. Brassard, C. Crépeau, R. Josza, A. Peres, and W. Wootters. Teleporting an unknown quantum state via dual classical and EPR channels. *Physical Review Letters*, 70:1895–1899, 1993.

[29] Dik Bouwmeester, Jian-Wei Pan, Klaus Mattle, Manfred Eibl, Harald Weinfurter, and Anton Zeilinger. Experimental quantum teleportation. *Nature*, 390:575–579, December 1997.

[30] A. Furusawa, J. L. Sørensen, S. L. Braunstein, C. A. Fuchs, H. J. Kimble, and E. S. Polzik. Unconditional quantum teleportation. *Science*, 282(5389):706–709, 1998.

[31] Chin-Wen Chou, Julien Laurat, Hui Deng, Kyung Soo Choi, Hugues de Riedmatten, Daniel Felinto, and H. Jeff Kimble. Functional quantum nodes for entanglement distribution over scalable quantum networks. *Science*, 316(5829):1316–1320, 2007.

[32] Z. Zhao, T. Yang, Y.A. Chen, A.N. Zhang, and J.W. Pan. Experimental realization of entanglement concentration and a quantum repeater. *Physical Review Letters*, 90(20):207901, 2003.

[33] A.K. Ekert. Quantum cryptography based on Bell's theorem. *Physical Review Letters*, 67(6):661–663, 1991.

[34] Charles H. Bennett, Herbert J. Bernstein, Sandu Popescu, and Benjamin Schumacher. Concentrating partial entanglement by local operations. *Physical Review A*, 53:2046, 1996.

[35] E.N. Maneva and J.A. Smolin. Improved two-party and multi-party purification protocols. *Contemporary Mathematics Series*, 305:203–212, 2000.

[36] W. Dür and H.J. Briegel. Entanglement purification and quantum error correction. *Rep. Prog. Phys*, 70:1381–1424, 2007.

[37] Jian-Wei Pan, Sara Gasparoni, Rupert Ursin, Gregor Weihs, and Anton Zeilinger. Experimental entanglement purification of arbitrary unknown states. *Nature*, 423:417–422, May 2003.

[38] L. Childress, J.M. Taylor, A.S. Sørensen, and M.D. Lukin. Fault-tolerant quantum communication based on solid-state photon emitters. *Physical Review Letters*, 96(7):70504, 2006.

[39] J.I. Cirac, P. Zoller, H.J. Kimble, and H. Mabuchi. Quantum state transfer and entanglement distribution among distant nodes in a quantum network. *Physical Review Letters*, 78(16):3221–3224, 1997.

[40] L.-M. Duan, B. B. Blinov, D. L. Moehring, and C. Monroe. Scalable trapped ion quantum computation with a probabilistic ion-photon mapping. *Quantum Information and Computation*, 4:165–173, 2004.

[41] S. J. van Enk, J. I. Cirac, and P. Zoller. Ideal quantum communication over noisy channels: A quantum optical implementation. *Phys. Rev. Lett.*, 78(22):4293–4296, June 1997.

[42] L.M. Duan, M.D. Lukin, J.I. Cirac, and P. Zoller. Long-distance quantum communication with atomic ensembles and linear optics. *Nature*, 414:413–418, 2001.

[43] W.J. Munro, K. Nemoto, and T.P. Spiller. Weak nonlinearities: a new route to optical quantum computation. *New Journal of Physics*, 7:137, May 2005.

[44] T. P. Spiller, Kae Nemoto, Samuel L. Braunstein, W. J. Munro, P. van Loock, and G. J. Milburn. Quantum computation by communication. *New Journal of Physics*, 8:30, February 2006.

[45] C.H. Bennett, G. Brassard, S. Popescu, B. Schumacher, J.A. Smolin, and W.K. Wootters. Purification of noisy entanglement and faithful teleportation via noisy channels. *Physical Review Letters*, 76(5):722–725, 1996.

[46] David Deutsch, Artur Ekert, Richard Jozsa, Chiara Macchiavello, Sandu Popescu, and Anna Sanpera. Quantum privacy amplification and the security of quantum cryptography over noisy channels. *Phys. Rev. Lett.*, 77(13):2818–2821, Sep 1996.

[47] J. Dehaene, M. Van den Nest, B. De Moor, and F. Verstraete. Local permutations of products of Bell states and entanglement distillation. *Physical Review A*, 67(2):22310, 2003.

[48] W. Dür, H.-J. Briegel, J. I. Cirac, and P. Zoller. Quantum repeaters based on entanglement purification. *Physical Review A*, 59(1):169–181, Jan 1999.

[49] L. Jiang, J.M. Taylor, N. Khaneja, and M.D. Lukin. Optimal approach to quantum communication using dynamic programming. *Proceedings of the National Academy of Sciences*, 104(44):17291, 2007.

[50] Raj Jain. *The Art of Computer Systems Performance Analysis*. John Wiley & Sons, 1991.

[51] Rodney Van Meter, Kae Nemoto, and William J. Munro. Communication links for distributed quantum computation. *IEEE Transactions on Computers*, 56(12):1643–1653, December 2007.